Plasma Passive Jamming for SAR Based on the Resonant Absorption Effect

Ruijia Wang, Xing Wang, Siyi Cheng, Yueyu Meng, Guanrong Zhang, and Yipeng Zhou

***Abstract*— The resonant absorption effect between plasma and electromagnetic waves makes the plasma a potential efficient passive jamming method for synthetic aperture radar. In this paper, the validity of plasma passive jamming is verified by comparing the echoes with and without plasma. First, the shift operator finite-difference time-domain method is utilized to numerically calculate the echoes from different plasma parameters. Then, the images of point target with and without plasma are obtained and compared. The image of point target with plasma is partly focused and the geometry character of point target is destructed. The simulation and analysis results validate the effectiveness of the proposed plasma passive jamming method.**

***Index Terms*— Passive jamming, plasma, resonant absorption, shift operator finite-difference time domain (SO-FDTD), synthetic aperture radar (SAR).**

I. Introduction

SYNTHETIC aperture radar (SAR) is widely used in various applications such as civil exploration and military surveillance due to its all-weather, long-time, and large-range detection capabilities [1]. Numerous jamming and electronic countermeasures methods have been developed to protect the vital targets against SAR reconnaissance. Based on the source of jamming power, the jamming is usually classified into active and passive jamming. The jamming signal of active jammer is directly generated with certain energy by the jammer. In contrast, the passive jamming usually scatters or reflects the incident signal to contaminate the target echoes.

Most of the research and literature to date have mainly focused on the active jamming. Various types of active jamming have been researched. In [1]–[4], the noise barrage jamming, a classical active jamming has been proposed. The deception jamming for normal stripe and squint SAR has been introduced in [5]–[7], and false target is formed in the image to mislead the image interpretation. Nevertheless, the passive jamming research for SAR is insufficient. The traditional passive reflecting jamming based on the corner reflector or scattering materials such as chaff is more effective for traditional target detection radar and pulse-Doppler radar than that of the SAR. The reason is that the SAR is a 2-D correlative system in both range direction and azimuth, while the traditional passive reflector only forms a stronger scatter in the resultant image. For example, the corner reflector is used for external calibration of SAR. Hence, using the passive jamming to form false targets or blur the protected target requires massive reflectors to form a matrix which is not flexible compared with active jamming.

However, the plasma has the potential to be an effective passive jamming method based on the capability of absorbing and distorting the target echo in a wide bandwidth. In the past year, considerable efforts have been made to study the plasma reflection efficiency, resonant absorbing, and other properties. In [8]–[10], the radar cross section (RCS) of a metal plate coated by collisional inhomogeneous plasmas has been researched. The propagation properties of electromagnetic (EM) waves in magnetized plasma have been introduced in [11]. The influence of plasma on the RCS descending of bistatic radar has been investigated in [12]. The interaction between the EM waves and plasma is severely affected by the plasma frequency and the collision frequency. With appropriate plasma parameter, Xu *et al.* [8] observed the distortion of radar echoes by plasma. Hence, the plasma was introduced for the first time as passive jamming method for traditional radar. Based on the resonant absorption effect, the main lobe energy of the target is decreased and dispersed in the adjacent sidelobe.

In this paper, the effectiveness of plasma passive jamming for SAR is evaluated. First, the plasma passive jamming principle is introduced. Then, the shift operator finite-difference time-domain (SO-FDTD) method is utilized to calculate the echoes from the plasma. Second, the point target imaging with plasma is simulated and the influence of point target with different plasma parameters is evaluated. The results demonstrate that the point target echoes are distorted and the point target image is partly focused with energy loss. Moreover, the geometrical characteristic of point target is destructed. Third, a scene is utilized to qualitatively demonstrate the influence of the proposed plasma passive jamming. The simulation results validate the effectiveness of the plasma passive jamming for SAR.

II. Plasma Passive Jamming Model for SAR Imaging

A. Principle of Plasma Passive Jamming

Fig. 1 shows the physical model of plasma passive jamming approximated with plasma stealth. The target is plasma coated

Manuscript received November 29, 2017; revised January 13, 2018 and January 29, 2018; accepted February 22, 2018. Date of publication March 13, 2018; date of current version April 10, 2018. This work was supported by the Chinese Aeronautic Foundation under Grant 20152096019. The review of this paper was arranged by Senior Editor D. A. Shiffler. *(Corresponding author: Ruijia Wang.)*

The authors are with Air Force Engineering University, Xi'an 710038, China (e-mail: wrjww08@163.com).

Color versions of one or more of the figures in this paper are available online at http://ieeexplore.ieee.org.

Digital Object Identifier 10.1109/TPS.2018.2811496

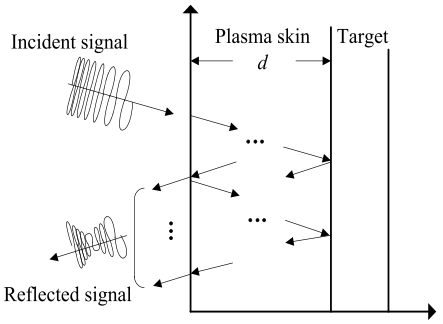

Fig. 1. Plasma passive jamming stretch.

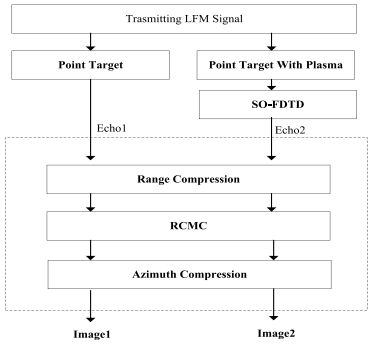

Fig. 2. Procedure of plasma passive jamming evaluation.

with a certain thickness and frequency. When the incident signal propagates in the plasma slab, it is divided into two parts. First part is directly reflected to the free space, while the second part is bounced multiple times in the plasma slab where the interactions between the penetrated signal and the plasma are based on the relative permittivity of plasma, which depends on the signal frequency. The liner frequency modulation (LFM) signal is usually used as the transmitting signal for SAR. The inner relationship between time and frequency of LFM signal will be distorted due to its multiple bouncing in plasma, which is called the resonant absorption effect. Hence, the echoes with strong resonant absorption effect can be adopted as a new passive jamming technology for SAR.

In theory, the electron density of collisional plasma is approximately stable [8]. Thus, the relative permittivity of plasma can be indicated as follows:

$$\varepsilon_r(\omega) = 1 + \frac{\omega_p^2}{\omega(j\upsilon_e - \omega)} \tag{1}$$

where ω and υ_e are the incident signal angular frequency and the electron collision frequency, respectively, while ω_p is the plasma frequency determined by the electron density and other parameters as shown in the following:

$$\omega_p = \sqrt{\frac{N_e e^2}{\varepsilon_0 m_e}} \tag{2}$$

where N_e is the electron density, ε_0 is the permittivity of free space, and e and m_e are the electron charge and mass, respectively.

B. SO-FDTD Method

In this paper, the SO-FDTD method is used to calculate the echoes from plasma coating targets. In [12]–[14], the SO-FDTD method is comprehensively researched for dispersive medium. According to the SO-FDTD method and Maxwell's equations, the relative permittivity can also be written as rational fractional function [12]

$$\varepsilon_r(\omega) = \frac{\sum_{n=0}^{N} p_n (j\omega)^n}{\sum_{n=0}^{N} q_n (j\omega)^n}. \tag{3}$$

The recurrence relation of electric field **E** can be indicated as follows:

$$E^{n+1} = \frac{1}{b_0}\left[\frac{a_0}{\varepsilon_0}D^{n+1} + \frac{a_1}{\varepsilon_0}D^n + \frac{a_2}{\varepsilon_0}D^{n-1} - b_1 E^n - b_2 E^{n-1}\right] \tag{4}$$

where

$$a_0 = q_0 + q_1\frac{2}{\Delta t} + q_2\left(\frac{2}{\Delta t}\right)^2, \quad a_1 = 2q_0 - 2q_2\left(\frac{2}{\Delta t}\right)^2$$
$$a_2 = q_0 - q_1\frac{2}{\Delta t} + q_2\left(\frac{2}{\Delta t}\right)^2, \; b_0 = p_0 + p_1\frac{2}{\Delta t} + p_2\left(\frac{2}{\Delta t}\right)^2$$
$$b_1 = 2p_0 - 2p_2\left(\frac{2}{\Delta t}\right)^2, \text{ and } b_0 = p_0 - p_1\frac{2}{\Delta t} + p_2\left(\frac{2}{\Delta t}\right)^2.$$

Meanwhile, comparing (3) with (1) implies $N = 2$ and $p_0 = \omega_p^2$, $p_1 = \upsilon_e$, $p_2 = 1$, $q_0 = 0$, $q_1 = \upsilon_e$, and $q_2 = 1$. Hence, the reflected echoes can be numerically calculated based on the recurrence equation.

C. SAR Imaging Model for Plasma Passive Jamming

When the resonant absorption frequency is in the bandwidth of the SAR, the echo will mismatch with the imaging filter. Thus, the target coated by plasma will defocus in the image. In this paper, the plasma passive jamming effectiveness is evaluated by comparing the images of point target with and without plasma. The procedure is shown in Fig. 2.

The transmitting LFM signal of SAR is as follows:

$$S(t) = \text{rect}\left(\frac{t}{T_r}\right)\exp(j2\pi f_0 t + j\pi K t^2) \tag{5}$$

where f_0, T_r, and K are the carrier frequency, the pulsewidth, and the frequency modulation rate, respectively. $S_{r_2}(t)$ and $S_{r_1}(t)$ are the echoes from the point target with and without plasma, respectively. Hence, the imaging process of each echo is as follows:

$$\begin{cases} S_{o_1}(\tau, \eta) = S_{r_1}(\tau, \eta) * h(\tau, \eta) \\ S_{o_2}(\tau, \eta) = S_{r_2}(\tau, \eta) * h(\tau, \eta) \end{cases} \tag{6}$$

where $h(\tau, \eta)$ is the 2-D match filter including the range and azimuth compression. Thus, the passive jamming effectiveness can be obtained by comparing the result in each imaging procedure.

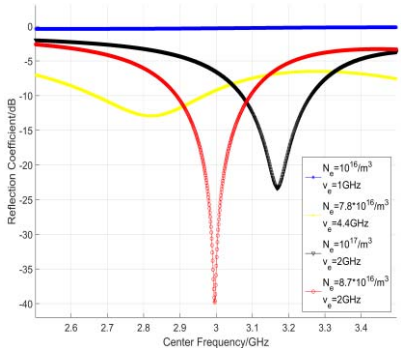

Fig. 3. Reflection coefficient in four plasma parameters.

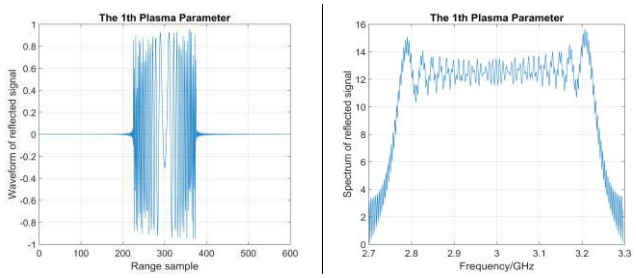

Fig. 4. Waveform and spectrum in the first plasma parameter.

III. Simulation and Analysis

The plasma parameters, such as the electron density and the collisional frequency, play a vital role in the effectiveness of resonant absorption. First, the parameter partially similar to that in [8] is adopted to show the resonant effect by calculating the reflection coefficient. Meanwhile, the thickness of four plasma parameters is 10 cm. The reflection coefficients with different plasma parameters are shown in Fig. 3.

A. Plasma Passive Jamming Waveform and Spectrum

The reflection coefficient curve will anomalously ascend or descend in some frequency bins when the reflection coefficient is strong. For example, the resonant absorption effect is weak when the plasma electronic density N_e is 1×10^{16} m^{-3} and collision frequency υ_e is 1 GHz. However, the resonant absorption effect is strong when N_e and υ_e are 8.7×10^{16} m^{-3} and 2 GHz, respectively.

Meanwhile, the four plasma parameters are utilized as plasma passive jamming parameters to compare the plasma passive jamming effect for point target. The carrier frequency f_0 is 3 GHz, the pulsewidth T_r is 2.5 μs, the frequency modulation rate K is 2×10^{14}, the oversampling rate is 1.2, and the bandwidth B is 500 MHz. It is assumed that the point target is located in the 300 range samples. The time-domain echoes and the spectrum are simulated by SO-FDTD numerical method as shown in Figs. 4–7.

Fig. 4 shows the waveform and spectrum corresponding with first plasma parameter where $N_e = 1 \times 10^{16}$ m^{-3} and $\upsilon_e = 1$ GHz. It can be seen that the echo in first plasma parameter is least effected. The waveform and spectrum corresponding to second plasma parameter are shown in Fig. 5,

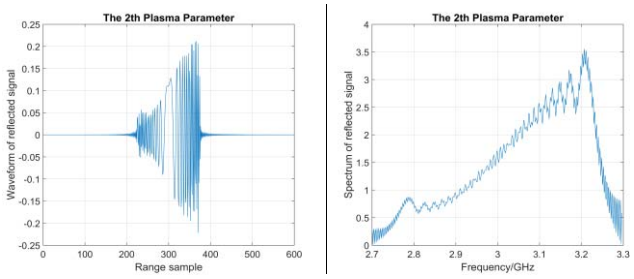

Fig. 5. Waveform and spectrum in the second plasma parameter.

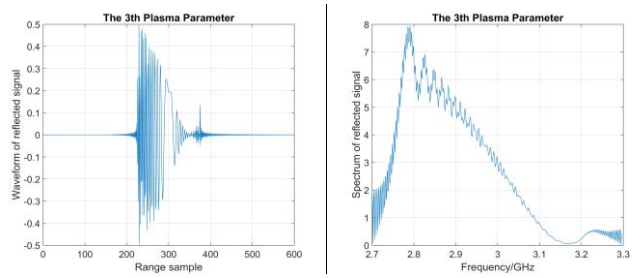

Fig. 6. Waveform and spectrum in the third plasma parameter.

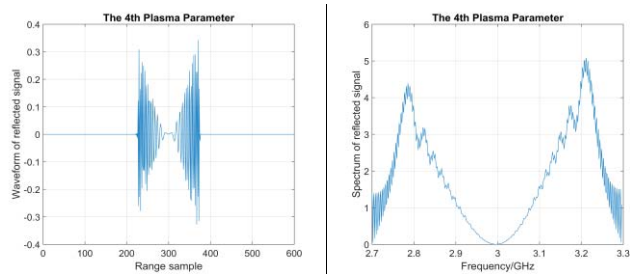

Fig. 7. Waveform and spectrum in the fourth plasma parameter.

where $N_e = 7.8 \times 10^{18}$ m^{-3} and $\upsilon_e = 4.4$ GHz. The waveform and spectrum ascend, respectively. Compared with Fig. 5, the waveform and spectrum corresponding to third plasma parameter descend in Fig. 6, where $N_e = 10 \times 10^{16}$ m^{-3} and $\upsilon_e = 2$ GHz. Fig. 7 shows that the waveform and spectrum, corresponding to fourth plasma parameter with $N_e = 8.7 \times 10^{16}$ m^{-3} and $\upsilon_e = 2$ GHz, first descend and then increase where a steep notch is made. The resonant absorption effect in the fourth plasma parameter is stronger than the other three parameters.

B. Plasma Passive Jamming Effect on Point Target Image

In order to evaluate the effectiveness of the plasma passive jamming, the point target image is simulated in four plasma parameters. Then, the range compression and the image results in different plasma parameters are compared with the result of point target without plasma. The image of point target without plasma is shown in Fig. 8.

Due to the resonant absorption effect, the echoes with plasma will partly mismatch with the range compression filter. The range compression results and the resultant images of point target in different plasma parameter are shown in Figs. 9–12.

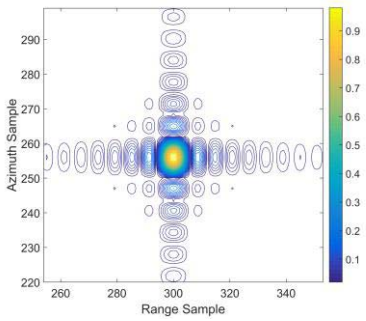

Fig. 8. Point target image without plasma.

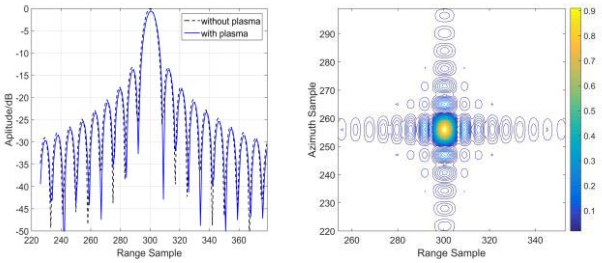

Fig. 9. Range compression and point target image in the first plasma parameter.

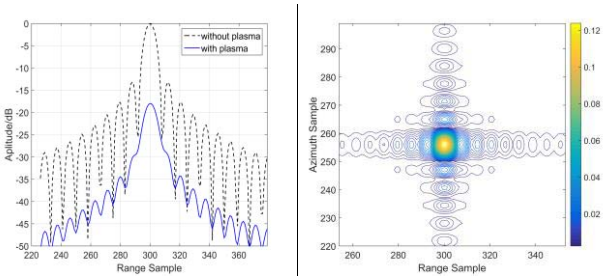

Fig. 10. Range compression and point target image in the second plasma parameter.

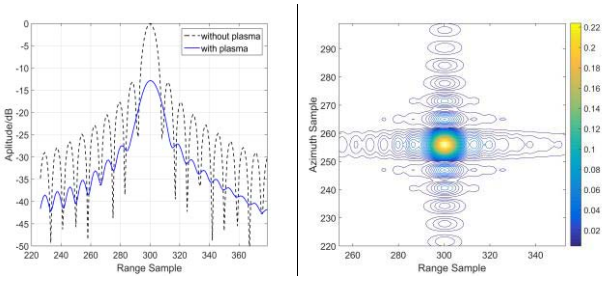

Fig. 11. Range compression and point target image in the third plasma parameter.

Detailed quantification evaluation indicators of point target image with and without plasma are calculated and listed in Table I, including the peak amplitude ratio (PAR), the correlation coefficient, the peak sidelobe ratio (PSLR), and the integrated sidelobe ratio (ISLR). The PAR presents the energy of point target, while the PSLR and ISLR present the geometry characteristic of the point target in the SAR image.

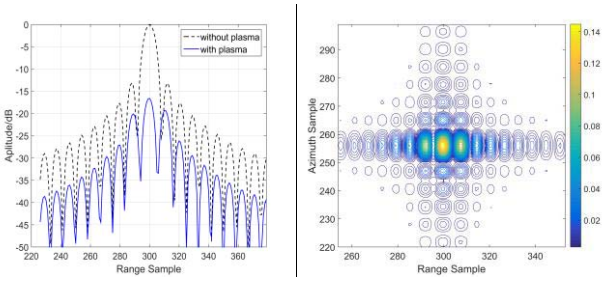

Fig. 12. Range compression and point target image in the fourth plasma parameter.

TABLE I

PLASMA PASSIVE JAMMING FOR POINT TARGET QUANTIFICATION EVALUATION RESULT

	PAR	r	PSLR(dB)	ISLR(dB)
Without Plasma	1	1	-13.36	-10.19
1*th* Plasma	0.876	0.928	-13.04	-10.14
2*th* Plasma	0.016	0.126	-9.61	-8.29
3*th* Plasma	0.052	0.229	-5.67	-7.53
4*th* Plasma	0.022	0.148	-2.83	-0.48

PAR: the peak amplitude ratio; r: the correlation coefficient; PSLR: the peak sidelobe ratio; ISLR: the integrated sidelobe ratio.

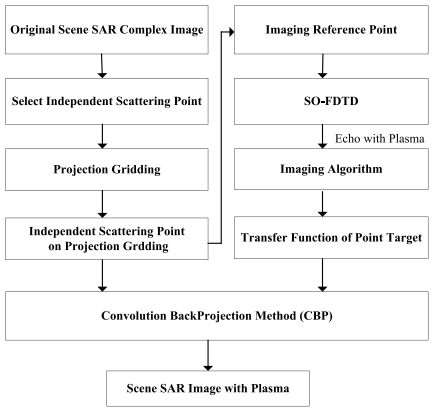

Fig. 13. Procedure of scene image simulation.

The correlation coefficients of the point target image with and without plasma show the image deterioration caused by plasma jamming.

Fig. 9 shows that the first plasma parameter has less jamming effect where the range compression of plasma is approximated with point target without plasma. The PAR of point target in the first plasma is 0.87, as shown in Table I. Both the PSLR and the ISLR approximate standard values of -13.3 and -10.1 dB, respectively, which means that the energy and the geometry characteristics of point target in the first parameter are maintained.

Figs. 10 and 11 show that the plasma jamming mismatch with the range compression match filter and the energy is attenuated in the image result. The PSLRs and the ISLRs in the second and the third plasma are both increased, meaning that the geometry characteristics of the main lobe and the sidelobe have changed. The gap between the main lobe and

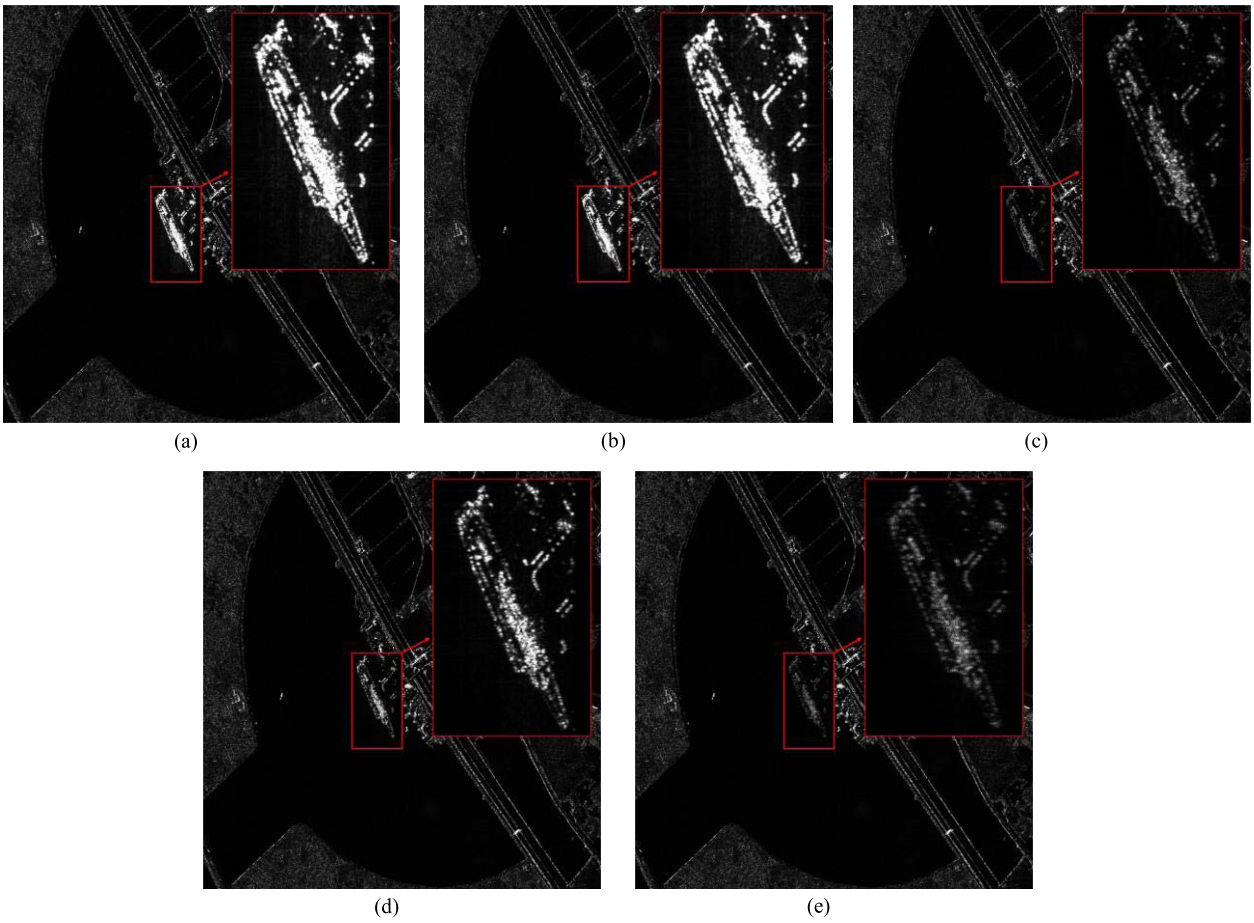

Fig. 14. Scene image. (a) Without plasma. (b) With the first plasma parameter. (c) With the second plasma parameter. (d) With the third plasma parameter. (e) With the fourth plasma parameter.

the sidelobe is fuzziness. The main lobe outline is changed compared with the point target without plasma. In the second plasma, the correlation coefficient is the smallest of the four plasma parameters.

Fig. 12 shows that the plasma jamming in the fourth plasma parameter has the strongest resonant absorption effect. Since the PSLR is increased to -2.83 dB, the plasma jamming is not only mismatched with the match filter but also forms two false targets in the original location of the sidelobe, which means that the energy in the main lobe is dispersed to the sidelobe. Meanwhile, the ISLR is the maximum of four plasma parameters and the geometry characteristic of the point target in the image is destructed. Based on the simulation result and quantification evaluation indicators, the fourth plasma parameter has the best jamming effect with the simulation condition. Hence, the plasma passive jamming for SAR is effective when the plasma parameter is optimal.

C. Plasma Passive Jamming Effect on Scene Image

In order to qualitatively validate the plasma jamming effect, a scene image is considered in which a ship is coated with plasma. The convolution backprojection (CBP) method is utilized to qualitatively simulate the scene image [15]. The simulation procedure is shown in Fig. 13.

First, independent scattering points are selected from the original scene image. The distance between the two independent scattering points is much greater than the SAR resolution. Under the condition of far-field, it is assumed that the independent scattering point is coated with the same and ideal plasma. Second, all independent scattering points are projected to the imaging gird. Then, the reference point target is selected and its echo is obtained by the SO-FDTD method. Third, the reference point target image is used as transfer function and the scene image is obtained utilizing the CBP method. The simulation scene images are shown in Fig. 14.

This four parameters are the same as described earlier. Fig. 14(b) shows that the jamming effect in the first plasma parameter is not prominent, and the brightness and the geometry characteristic of the ship with plasma are barely changed. However, in Fig. 14(c)–(e), the ship brightness attenuation is significant. In particular, the ship outline in Fig. 14(e) is blurred compared with Fig. 14, which validates the plasma passive jamming.

IV. Conclusion

In this paper, the effectiveness of the plasma passive jamming for SAR is verified. The SO-FDTD method is used to numerically calculate the echoes from different plasma

parameters, and the resultant images of point target with and without plasma are obtained. The comparison analysis shows that the waveform and the spectrum of echoes from target coated by plasma are distorted due to the resonant absorption effect.

Hence, the plasma has negative influence on the range compression and imaging. When the plasma parameter is optimal, the range compression amplitude of point target is not only degraded, but also the geometry characteristic of point target is destructed that may mislead the SAR image interpretation. The work presented in this paper suggests that the plasma passive jamming can be a promising jamming method to SAR for excellent jamming effect.

REFERENCES

[1] R. S. Harness and M. C. Budge, "A study on SAR noise jamming and false target insertion," in *Proc. IEEE SOUTHEASTCON*, Lexington, KY, USA, Mar. 2014, pp. 1–8.

[2] K. Dumper, P. S. Cooper, A. F. Wons, C. J. Condley, and P. Tully, "Spaceborne synthetic aperture radar and noise jamming," in *Proc. Radar Syst.*, 1997, pp. 411–414.

[3] Z. Shenghua, X. Dazhuan, J. Xueming, and H. Hua, "A study on active jamming to synthetic aperture radar," in *Proc. 3rd Int. Conf. Comput. Electromagn. Appl. (ICCEA)*, Nov. 2004, pp. 403–406.

[4] D.-H. Dai, X. F. Wu, X.-S. Wang, and S.-P. Xiao, "SAR active-decoys jamming based on DRFM," in *Proc. IET Int. Conf. Radar Syst.*, Edinburgh, U.K., Oct. 2007, pp. 1–4.

[5] L. Huang, C. M. Dong, Z. Shen, and G. Zhao, "The influence of rebound jamming on SAR GMTI," *IEEE Geosci. Remote Sens. Lett.*, vol. 12, no. 2, pp. 399–403, Feb. 2015.

[6] N. S. Tezel and S. Paker, "Inserting moving targets to polarimetric SAR image by self deception jamming," in *Proc. 7th Eur. Conf. Synth. Aperture Radar*, Friedrichshafen, Germany, Jun. 2008, pp. 1–3.

[7] B. Zhao, F. Zhou, and Z. Bao, "Deception jamming for squint SAR based on multiple receivers," *IEEE J. Sel. Topics Appl. Earth Observ. Remote Sens.*, vol. 8, no. 8, pp. 3988–3998, Aug. 2015.

[8] J. Xu, B. Bai, C. Dong, Y. Zhu, Y.-Y. Dong, and G. Zhao, "A novel plasma jamming technology based on the resonance absorption effect," *IEEE Antennas Wireless Propag. Lett.*, vol. 16, pp. 1056–1059, 2017.

[9] B. Chaudhury and S. Chaturvedi, "Three-dimensional computation of reduction in radar cross section using plasma shielding," *IEEE Trans. Plasma Sci.*, vol. 33, no. 6, pp. 2027–2034, Dec. 2005.

[10] B. Chaudhury and S. Chaturvedi, "Study and optimization of plasma-based radar cross section reduction using three-dimensional computations," *IEEE Trans. Plasma Sci.*, vol. 37, no. 11, pp. 2116–2127, Nov. 2009.

[11] P. Li and L. J. Jiang, "Simulation of electromagnetic waves in the magnetized cold plasma by a DGFETD method," *IEEE Antennas Wireless Propag. Lett.*, vol. 12, pp. 1244–1247, 2013.

[12] W. Liu *et al.*, "The influence of plasma induced by α-particles on the radar echoes," *IEEE Trans. Plasma Sci.*, vol. 43, no. 1, pp. 405–413, Jan. 2015.

[13] L.-X. Ma, H. Zhang, Z. Li, and C.-X. Zhang, "Improved finite difference time-domain method for anisotropic magnetised plasma based on shift operator," *IET Microw., Antennas Propag.*, vol. 4, no. 9, pp. 1442–1447, 2010.

[14] F. Mirhosseini and B. Colpitts, "Simulating RCS of dispersive media using SO-FDTD-DPW method," in *Proc. IEEE 28th Can. Conf. Electr. Comput. Eng. (CCECE)*, Halifax, NS, Canada, May 2015, pp. 513–518.

[15] M. D. Desai and W. K. Jenkins, "Convolution backprojection image reconstruction for spotlight mode synthetic aperture radar," *IEEE Trans. Image Process.*, vol. 1, no. 4, pp. 505–517, Oct. 1992.

Ruijia Wang was born in 1990. He received the B.S. degree from the University of Electronic Science and Technology of China, Chengdu, China, in 2012, and the M.S. degree from Air Force Engineering University, Xi'an, China, in 2015, where he is currently pursuing the Ph.D. degree.

His current research interests include synthetic aperture radar jamming and antijamming technologies.

Xing Wang was born in 1965. He received the Ph.D. degree from Northwestern Polytechnical University, Xi'an, China, in 2011.

He is currently a Professor with the Aeronautics Engineering College, Air Force Engineering University, Xi'an. His current research interests include electronic countermeasures.

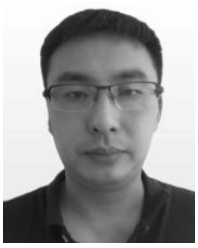

Siyi Cheng was born in 1980. He received the Ph.D. degree from Air Force Engineering University, Xi'an, China, in 2007.

He is currently an Associate Professor with the Aeronautics Engineering College, Air Force Engineering University. His current research interests include electronic countermeasures.

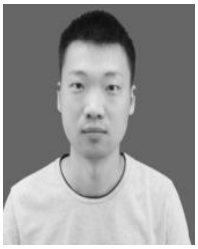

Yueyu Meng was born in 1990. He received the B.S. and M.S. degrees from Air Force Engineering University, Xi'an, China, in 2012 and 2015, respectively, where he is currently pursuing the Ph.D. degree.

His current research interests include plasma stealth technology and left-handed materials.

Guanrong Zhang was born in 1981. He received the M.S. degree from Air Force Engineering University, Xi'an, China, in 2012.

He is currently an Associate Professor with the Aeronautics Engineering College, Air Force Engineering University. His current research interests include electronic countermeasures.

Yipeng Zhou was born in 1992. He received the B.S. and M.S. degrees from Air Force Engineering University, Xi'an, China, in 2014 and 2017, respectively, where he is currently pursuing the Ph.D. degree.

His current research interests include electronic countermeasures.